Kidney International, Vol. 55 (1999), pp. 1683–1695

GENETIC DISORDERS – DEVELOPMENT

The renal lesions that develop in neonatal mice during angiotensin inhibition mimic obstructive nephropathy

Yoichi Miyazaki, Shinya Tsuchida, Agnes Fogo, and Iekuni Ichikawa

Departments of Pediatrics, Pathology, and Medicine, Vanderbilt University Medical Center Nashville, Tennessee, USA

The renal lesions that develop in neonatal mice during angiotensin inhibition mimic obstructive nephropathy.

Background. Inhibition of angiotensin action, pharmacologically or genetically, during the neonatal period leads to renal anomalies involving hypoplastic papilla and dilated calyx. Recently, we documented that angiotensinogen (*Agt* −/−) or angiotensin type 1 receptor nullizygotes (*Agtr1* −/−) do not develop renal pelvis nor ureteral peristaltic movement, both of which are essential for isolating the kidney from the high downstream ureteral pressure. We therefore examined whether these renal anomalies could be characterized as "obstructive" nephropathy.

Methods. Agtr1 −/− neonatal mice were compared with wild-type neonates, the latter subjected to surgical complete unilateral ureteral ligation (UUO), by analyzing morphometrical, immunohistochemical, and molecular indices. *Agtr1* −/− mice were also subjected to a complete UUO and were compared with wild-type UUO mice by quantitative analysis. To assess the function of the urinary tract, baseline pelvic and ureteral pressures were measured.

Results. The structural anomalies were qualitatively indistinguishable between the *Agtr1* −/− without surgical obstruction versus the wild type with complete UUO. Thus, in both kidneys, the calyx was enlarged, whereas the papilla was atrophic; tubulointerstitial cells underwent proliferation and also apoptosis. Both were also characterized by interstitial macrophage infiltration and fibrosis, and within the local lesion, transforming growth factor-β1, platelet-derived growth factor-A, and insulin-like growth factor-1 were up-regulated, whereas epidermal growth factor was down-regulated. Moreover, quantitative differences that exist between mutant kidneys without surgical obstruction and wild-type kidneys with surgical UUO were abolished when both underwent the same complete surgical UUO. The hydraulic baseline pressure was always lower in the pelvis than that in the ureter in the wild type, whereas this pressure gradient was reversed in the mutant.

Conclusion. The abnormal kidney structure that develops in neonates during angiotensin inhibition is attributed largely to "functional obstruction" of the urinary tract caused by the defective development of peristaltic machinery.

Key words: gene targeting, unilateral ureteral obstruction, angiotensin converting enzyme inhibitor, renal pelvis, ureter.

Received for publication August 21, 1998
and in revised form December 8, 1998
Accepted for publication December 16, 1998

Considerable evidence has amassed to suggest that angiotensin II plays an important regulatory role in the development of the kidney. Indeed, renin and angiotensin are up-regulated in the kidney during the perinatal period [1–4], and pharmacological blockade of the renin-angiotensin system in neonatal rats induces gross abnormalities in the structure and function of the kidney [5, 6]. Moreover, recent gene targeting studies revealed that mice lacking angiotensinogen [7–9], angiotensin-converting enzyme (ACE) [10–12], or type 1 receptor [13] develop major abnormalities in renal morphogenesis, which become evident shortly after birth. However, the mechanistic explanation has not been provided linking the lack of angiotensin action and the abnormal renal development.

The renal pelvis, an organ unique to mammals, consists of a smooth muscle layer extending from the renal parenchyma to the downstream ureter. The pelvis develops immediately after birth when the renal system faces dual challenges of achieving some 50-fold increase in urine production to eliminate nitrogenous wastes entirely through the kidney [14] and, at the same time, of establishing the mechanism by which the high urine output is matched by efficient removal of urine from the kidney. Under the control of its pacemaker cells, the pelvis initiates peristaltic movements to transfer urine rapidly from the kidney to the ureter [15, 16]. Of note, angiotensin type 1 receptor is intensely expressed along the pelvic smooth muscle [4, 17], and angiotensin can stimulate contraction of the pelvic smooth muscle in *in vitro* settings [18].

In a recent study, we found that mice lacking either angiotensinogen (*Agt* −/−) or both angiotensin type 1 A and 1B receptors (*Agtr1* −/−) fail to develop a renal pelvis or ureteral peristaltic movement [4]. The ability of angiotensin to induce the pelvis directly was demonstrated in an organ culture system in which treatment with angiotensin induced the characteristic smooth muscle layer, which is missing in homozygous mutants. We therefore speculated that the structural anomalies that develop shortly after birth in animals, which are subjected

to pharmacological or genetic inhibition of angiotensin action, specifically atrophic papilla and dilated calyx, are equivalent to an obstructive nephropathy in nature.

In this study, we measured several structural and molecular indices in *Agtr1* −/− kidneys and found that morphometrically, immunohistochemically, molecularly, and otherwise, the nature of the renal parenchymal damage of *Agtr1* −/− mice is qualitatively indistinguishable from that of wild-type mice that have been subjected to a complete surgical unilateral ureteral ligation (UUO). Moreover, the quantitative difference that existed between *Agtr1* −/− mice without surgical obstruction and wild-type mice with UUO was essentially abolished when both had undergone the same complete surgical UUO, indicating that the abnormal kidney structure of angiotensin type 1 receptor null mutants is attributed largely to "functional obstruction" of the urinary tract caused by the defective development of peristaltic machinery.

METHODS

Animals

To obtain pups lacking both angiotensin type 1A (AT1A) and type 1B (AT1B) receptors, double heterozygous null mutants (*Agtr1a* +/−, *Agtr1b* +/−) on a mixed 129/Ola and C57BL/6 genetic background were interbred as described previously [4, 13]. The offspring that carried the genotype +/+ or *Agtr1a* −/− and *Agtr1b* −/− (abbreviated as *Agtr1* −/−), which had neither 1A nor AT1B receptors, were used in this study. The *Agtr1* genotype was determined by Southern blot analysis on DNA isolated from tail biopsies.

Surgical preparation of unilateral ureteral obstruction

Some animals were subjected to experimental ureteral obstruction. Under anesthesia by intraperitoneal injection of sodium pentobarbital (60 mg/kg body wt), the left ureters of 16-day-old mice were ligated with 6-0 silk and cut between the two ligated points, whereas in sham operation, the ureter was identified and left undisturbed. After the pups recovered from anesthesia, they were returned to their mother. At five days after surgery, obstructed kidneys were harvested and subjected to the analyses specified later here ($N = 6$, *Agtr1* +/+ with sham operation, $N = 6$ for *Agtr1* −/− with sham operation, $N = 6$ for *Agtr1* +/+ with UUO, and $N = 5$ for *Agtr1* −/− with UUO).

Inhibition of angiotensin-converting enzyme during the neonatal period

Wild-type mice were injected subcutaneously with ACE inhibitor (imidapril, 20 mg/kg/day) in a volume of 10 μl/g. Injections started at the day of birth and continued until 5 ($N = 5$) or 21 days of age ($N = 5$). As a control, mice were injected with an equal volume of saline for 5 ($N = 5$) or 21 days ($N = 5$). These mice were then analyzed for gross morphology of the renal pelvis and renal histology as specified later in this article.

Assessment of renal pelvic and ureteral pressure

Mice were anesthetized with an intraperitoneal injection of 60 mg/kg body wt sodium pentobarbital. Following tracheostomy, a polyethylene catheter (PE-10) was placed into the right jugular vein for continuous infusion of saline (2 ml/hr). After a midline incision of the abdomen, the dome of the bladder was punctured with a 22 gauge needle to allow free urine outflow. The fat pad surrounding the kidney was anchored in order to immobilize the left renal pelvis, and the fat pad surrounding the pelvis was gently removed. The hydraulic pressure within the urinary tract was recorded with a continuous recording, servo-null micropipette transducer system (model 4A; Instrumentation for Physiology and Medicine, San Diego, CA, USA) as described previously [19].

Histological study

Kidneys were fixed with 4% buffered paraformaldehyde for four hours, dehydrated, embedded in paraffin, sectioned at 4 μm, and subjected to the following histological examinations.

Immunohistochemistry. Rat antimouse F4/80 (1:300 dilution; Selotec, Oxford, UK), mouse antihuman α-smooth muscle actin (SMA; Dako, Carpinteria, CA, USA), goat antihuman insulin-like growth factor (IGF1; 1:200 dilution; R&D System, Minneapolis, MN, USA), and rabbit antimouse epidermal growth factor (EGF; 1:4000 dilution; Sigma, St. Louis, MO, USA) were used as primary antibodies.

The ABC method was applied for immunostaining with F4/80, IGF1, or EGF antibody. After quenching with 3% hydrogen peroxide in methanol for 10 minutes and preincubation in blocking solution of Vectastain® ABC kit (Vector, Burlingame, CA, USA) for two hours, sections were incubated with primary antibody for 16 hours at 4°C. After washing with phosphate-buffered saline (PBS), the sections were incubated with biotinylated second antibody (Vector) for 30 minutes and then incubated in avidin-biotin complex peroxidase solution (Vector) for one hour at room temperature. Development was accomplished with incubation in peroxidase substrate (Research Genetics, Huntsville, AL, USA) for three to five minutes at room temperature.

For immunostaining with α-SMA antibody, the sections were incubated with primary antibody conjugated with horseradish peroxidase for one hour at room temperature and developed in peroxidase substrate (Research Genetics), following the manufacturer's protocol.

Morphometric analyses of the papilla to calyx ratio, proliferating cells, apoptotic cells, macrophage infiltration, and α-smooth muscle actin expression. To measure

the papilla to calyx ratio in the kidney specimen, three nonadjacent coronal sections of the kidneys at the level of the renal hilum were traced with the aid of camera lucida attachment and scanned with JX-330M scanner (Sharp Co., Osaka, Japan). The area of the papilla or maximum calyceal space was quantitated using the National Institutes of Health Image program. The percentages of the papillary area to the papillary plus caliceal area were averaged for each kidney, and then the values from six kidneys were further averaged.

The bromodeoxyuridine (BrdU) labeling method was used to identify proliferating cells. One day before sacrifice, mice were given three intraperitoneal injections of BrdU (0.1 mg/g body wt; Boehringer Mannheim, Mannheim, Germany) at nine-hour intervals. Two hours after the last injection, kidneys were removed and processed as described earlier here. Immunostaining for BrdU was performed with anti-BrdU antibody (Calbiochem, Cambridge, MA, USA) following the manufacturer's protocol. For individual kidneys, eight nonoverlapping fields within either the cortex or medulla were examined under high magnification (×400), and the number of BrdU-positive nuclei was averaged for each field (nuclei/400× field), and the values from six kidneys were then averaged.

The terminal deoxy transferase uridine triphosphate nick end-labeling (TUNEL) method was employed to detect apoptotic cells according to the protocol that Gavrieli, Sherman and Ben-Sasson described [20]. After treatment with 2.5 μg/ml of proteinase K (Sigma) for 10 minutes, sections were incubated with 0.01 nmol/μl of digoxigenin-conjugated dUTP (Boehringer Mannheim) and 0.25 U/μl terminal transferase (Boehringer Mannheim) for 16 hours at 4°C. The slides were washed extensively with water and a solution containing 0.1 M maleic acid and 0.15 M NaCl (pH 7.5). A digoxigenin antibody alkaline phosphatase-conjugated Fab fragment (Boehringer Mannheim) was used for detection of the digoxigenin incorporated into the DNA. Rat thymus tissues harvested after irradiation were used for positive control. The number of TUNEL-positive cells was examined in the cortical or medullary region, normalized by the area measured planimetrically using the Micro-Plan II image analysis system, and expressed as TUNEL-positive cells/mm^2.

Macrophage infiltration was determined by the number of cells within the cortex or medulla, which were stained positively with F4/80 antibody. For individual kidneys, eight nonoverlapping fields within either the cortex or medulla were examined under high magnification (×400), and the numbers of positive cells were averaged for each field (nuclei/400× field), and the values from six kidneys were then averaged.

Expression of α-SMA in the interstitium was assessed semiquantitatively by immunoreactivity for α-SMA. The expression score from 0 to 3 was based on the intensity and distribution of α-SMA immunoreactivity, in which 0 represents no expression, 1 represents mild expression, 2 represents moderate expression, and 3 represents severe expression, according to the method of Kaneto, Morrissey and Klahr [21]. In each section, the score was counted in eight random fields under high magnification, and the score was averaged for each field.

In situ hybridization for transforming growth factor-β1 and platelet-derived growth factor-A. Mouse *Sma* I-*Sma* I fragment of TGF-β1 cDNA clone [7, 22] and *Pst* I-*EcoR* I fragment of PDGF-A cDNA clone [7, 23] were used as templates to synthesize ^{35}S-labeled cRNA antisense and sense probe by *in vitro* transcription kit (Ambion, Austin, TX, USA) following the manufacturer's protocol. These probes cover 0.97 kb (421 to 1395 bp) and 0.56 kb (345 to 906 bp), respectively, of mouse transforming growth factor-β1 (TGF-β1) and platelet-derived growth factor-A (PDGF-A) cDNA.

The protocol for *in situ* hybridization was a slight modification of one described previously [7]. Sections were refixed in 4% paraformaldehyde (PFA) for 20 minutes, washed in PBS, and then treated with 2 μg/ml proteinase K for five minutes. Subsequently, sections were twice acetylated with 0.4% (vol/vol) acetic anhydride in 0.1 M triethanolamine for 10 minutes. After rinsing in PBS, sections were dehydrated through graded alcohols and air dried. Sections were covered with 100 μl of hybridization mixture containing ^{35}S-labeled cRNA probe (2×10^4 cpm/ml), 50% deionized formamide, 10% dextran sulfate, 8 mM dithiothreitol (DTT), 0.2 mg/ml tRNA, 0.02% Ficoll, and 0.02% bovine serum albumin and were then incubated overnight at 50°C in a sealed, humidified container. After hybridization, the slides were washed in 50% formamide, 2 × standard saline citrate (SSC), and 100 mM DTT at 65°C for 20 minutes and were treated with 20 μg/ml RNase A at 37°C for 30 minutes. Sections were washed in 2 × SSC, followed by 0.1 × SSC at 65°C, dehydrated through graded alcohols with 0.3 M ammonium acetate, and air dried. They were dipped in photographic emulsion (Ilford K2 emulsion; Ilford Ltd., Essex, UK), diluted in 2% glycerol solution, air dried, and exposed at 4°C for 10 to 14 days. After development with D-19 developer, the slides were counterstained with 0.1% toluidine blue.

Northern blot analyses for transforming growth factor-β1, platelet-derived growth factor-A, epidermal growth factor, and insulin-like growth factor 1 mRNA

The cDNA probes for mouse TGF-β1, PDGF-A, and EGF were the 0.97 kb *Sma* I-*Sma* I fragment [22], the 0.56 kb *Pst* I-*EcoR* I fragment [23], and 0.78 kb *Apa* I-*Spe* I fragment of EGF cDNA [24], respectively. The cDNA probe for mouse IGF1 was synthesized and amplified from mouse kidney total RNA using oligonucleotide primers as follows: 5′ primer, 5′-AGCTCCACCACAG CTGGACCA-3′: 3′ primer, 5′-ACGGATAGAGCGGG

CTGCTTTTGAT-3′ [25]. The amplified fragment was subcloned into PCR®II-TOPO (Invitrogen, Carlsbad, CA, USA), and the specific insert was used as the IGF1 probe.

Twenty micrograms of whole kidney RNAs were electrophoresed in 1% agarose, 2.2 M formaldehyde, and MOPS buffer gel, transferred to a nylon membrane (Hybond-N+; Amersham Life Science Inc., Arlington Heights, IL, USA) and hybridized with ^{32}P-labeled probe. Following hybridization, the membranes were washed in 2 × SSC in 0.1% sodium dodecyl sulfate (SDS) for 10 minutes at room temperature twice and then 0.2 × SSC in 0.1% SDS for 15 minutes at 65°C twice. The membrane was rehybridized with a human glyceraldehyde 3-phosphate dehydrogenase (GAPDH) cDNA probe (Clontech, Palo Alto, CA, USA) as a control for RNA loading. The hybridization signal of each mRNA was detected by autoradiography and scanned with JX-330M scanner (Sharp Co.), and semiquantitated using National Institutes of Health Image program.

Statistical analysis

Data are presented as means ± SE. Statistical analysis was performed using analysis of variance followed by Bonferroni test for multiple comparisons.

RESULTS

Measurement of pressure within the pelvis and ureter

Previously, we measured peristaltic pressure within the pelvis of wild-type and *Agtr1* −/− mice and found that in wild-type mice, the renal pelvic pressure exhibits slow rhythmic pulsatile changes with constant frequency, whereas the regular contraction of the renal pelvis is absent in mutant mice. This time, we measured the pelvic pressure and the downstream ureteral pressure at the same time in the same mice (Fig. 1). Although the values for pelvic and ureteral pressure differ among mice within each group, the baseline pressure is always lower in the pelvis than in the distal ureter in the wild type (on average by 7.0 ± 0.3 mm Hg, $N = 4$), whereas this pressure gradient is reversed in mutants (on average by 1.2 ± 0.3 mm Hg, $N = 4$; Fig. 1).

Gross histological examination

Evaluation of coronal sections reveals that *Agtr1* −/− kidneys have distinctive pathologic lesions, for example, hypoplastic papilla, tubular atrophy and dilation, and interstitial fibrosis, that is, features that are similar to those in *Agtr1* +/+ kidneys with surgical UUO (Fig. 2). Morphometrical analysis shows that the papilla to calyx ratio is significantly lower in *Agtr1* −/− kidneys (*Agtr1* +/+ kidneys, 84.0 ± 1.5%; *Agtr1* −/− kidneys, 54.5 ± 8.2, $N = 6$, $P < 0.01$), although the ratio is higher than that in *Agtr1* +/+ kidneys with surgical UUO (22.5 ± 2.3%, $P < 0.01$, $N = 6$).

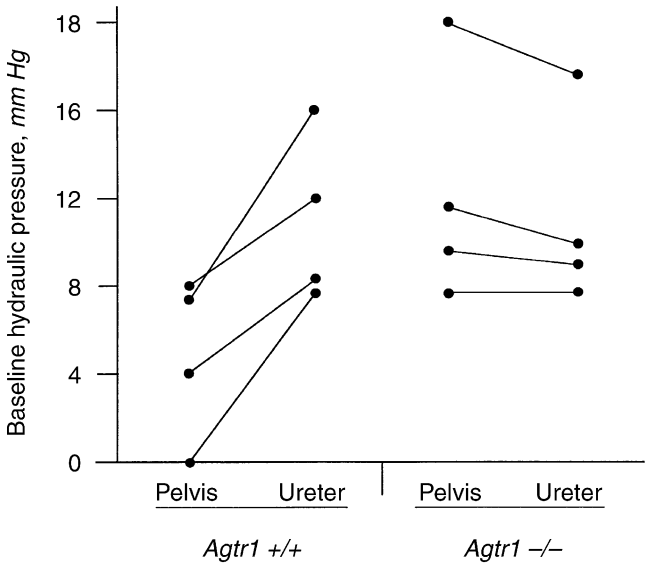

Fig. 1. Renal pelvic and ureteral pressure in *Agtr1* +/+ and *Agtr1* −/−. Intrarenal pelvic and intraureteral pressures were monitored in the same mice by the servo-nulling micropuncture method. In all of the wild-type mice examined ($N = 4$), baseline pressure in the pelvis was lower than that in the downstream ureter, whereas this baseline pressure gradient was reversed in *Agtr1* −/− mice ($N = 4$).

Examination for cell proliferation, apoptotic cells, macrophage infiltration, and α-smooth muscle actin expression in the interstitium

Bromodeoxyuridine-positive nuclei are observed mainly in tubules and, to a lesser extent, in the interstitium in all preparations (Fig. 3). As shown in Figure 4, for the cortex, a high level of BrdU incorporation is observed in wild-type kidneys at the age of 21 days, as in the *Agtr1* −/− kidneys (*Agtr1* +/+, 94.0 ± 9.7/400× field, $N = 6$; *Agtr1* −/−, 119.6 ± 9.2/400× field, $N = 6$). By contrast, in the medulla, BrdU-positive cells are significantly higher in number in the *Agtr1* −/− kidneys (94.2 ± 3.2/400× field, $N = 6$) than in wild-type kidneys (25.3 ± 2.5/400× field, $N = 6$, $P < 0.001$), and comparable only to wild-type kidneys with surgical UUO (112.5 ± 3.2/400× field, $N = 6$).

TUNEL staining revealed that, in the wild type, there are only few apoptotic cells in the kidney (cortex, 0.3 ± 0.1/mm^2; medulla, 1.0 ± 0.3/mm^2), whereas in the *Agtr1* −/−, the apoptotic cell number is distinctively increased along the dilated tubules in the cortex and medulla (cortex, 6.5 ± 1.2/mm^2, $P < 0.05$; medulla, 10.9 ± 1.3/mm^2, $P < 0.05$; Figs. 3 and 4). High-power views of Figure 3 E–G were also presented by Miyazaki et al [4]. Surgical complete UUO led to increased apoptotic cells in *Agtr1* +/+ kidneys (cortex, 20.5 ± 3.7, $P < 0.001$; medulla, 26.0 ± 2.9/mm^2, $P < 0.001$) in a region similar to *Agtr1* −/− kidneys in a degree greater than the latter ($P < 0.01$).

F4/80-positive cells were present primarily in the renal interstitium that directly surrounds renal tubules (Fig.

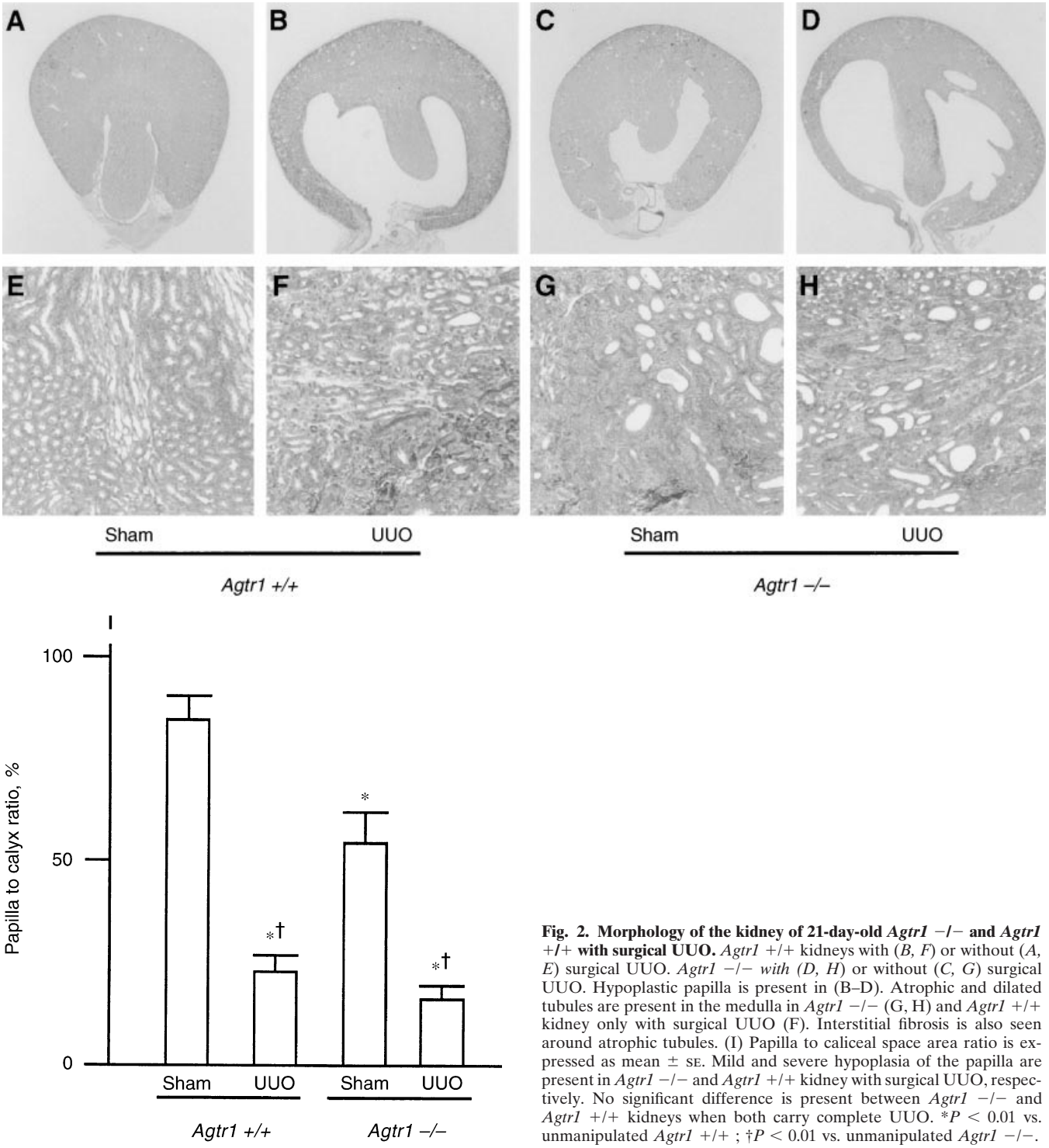

Fig. 2. Morphology of the kidney of 21-day-old *Agtr1* −/− and *Agtr1* +/+ with surgical UUO. *Agtr1* +/+ kidneys with (*B, F*) or without (*A, E*) surgical UUO. *Agtr1* −/− *with (D, H*) or without (*C, G*) surgical UUO. Hypoplastic papilla is present in (B–D). Atrophic and dilated tubules are present in the medulla in *Agtr1* −/− (G, H) and *Agtr1* +/+ kidney only with surgical UUO (F). Interstitial fibrosis is also seen around atrophic tubules. (I) Papilla to caliceal space area ratio is expressed as mean ± SE. Mild and severe hypoplasia of the papilla are present in *Agtr1* −/− and *Agtr1* +/+ kidney with surgical UUO, respectively. No significant difference is present between *Agtr1* −/− and *Agtr1* +/+ kidneys when both carry complete UUO. *$P < 0.01$ vs. unmanipulated *Agtr1* +/+ ; †$P < 0.01$ vs. unmanipulated *Agtr1* −/−.

3). The *Agtr1* −/− kidney has a significantly greater degree of macrophage infiltration (cortex, 77.7 ± 5.1/400× field; medulla, 74.5 ± 9.1/400× field) than that of the wild type (cortex, 26.0 ± 4.3/400× field, $P < 0.01$; medulla, 34.5 ± 4.0/400× field, $P < 0.01$; Fig. 4). Surgical UUO in the wild type increases F4/80-positive cells in both cortex and medulla to levels (cortex, 97.8 ± 8.5/400× field; medulla, 83.8 ± 8.6/400× field) that are quantitatively similar to those in *Agtr1* −/− kidneys.

Immunoreactivity of α-SMA is present homogeneously in the interstitium that surrounds tubules in the cortex and intensely in the inner stripe of outer medulla

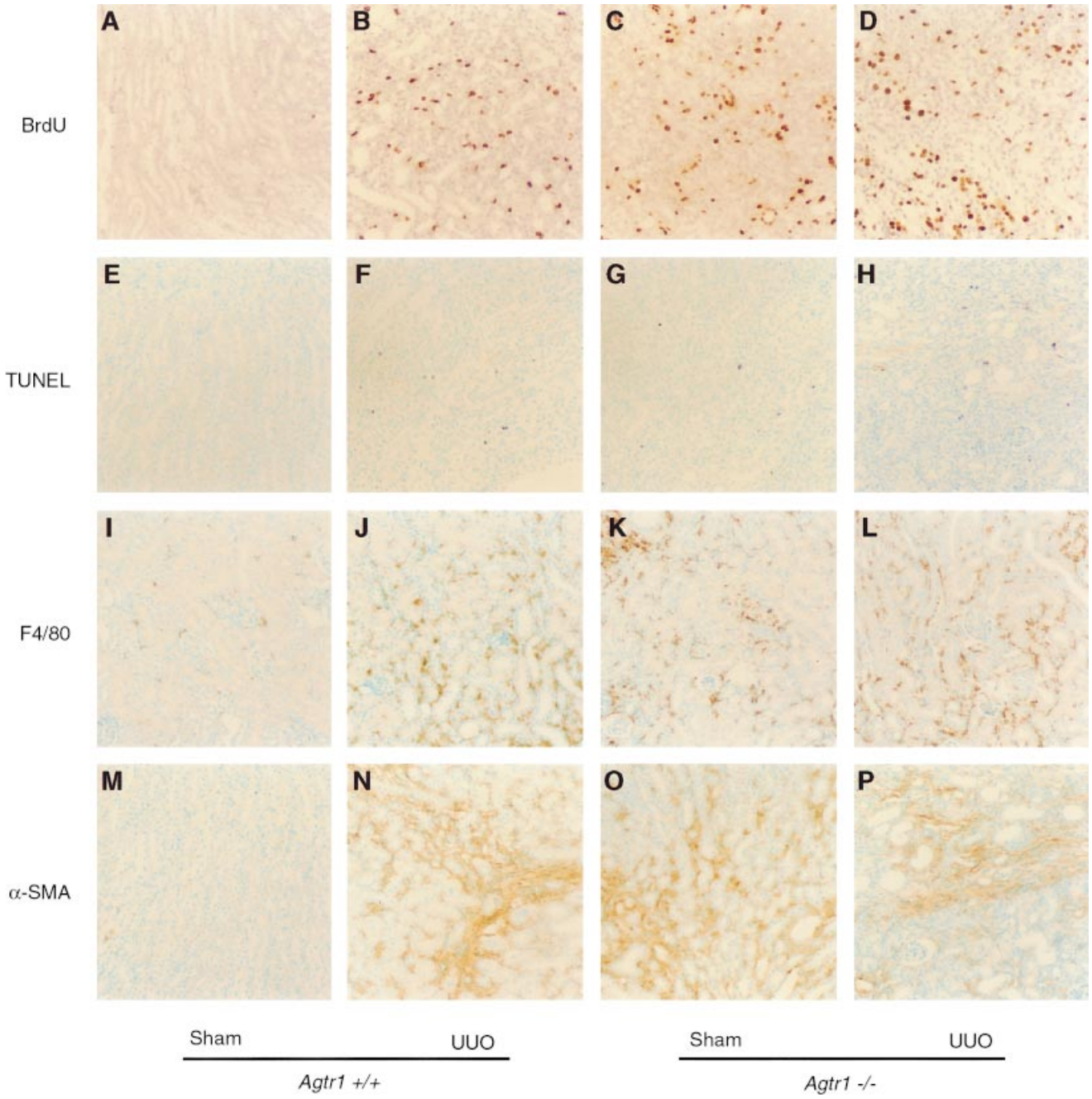

Fig. 3. Detection of proliferating cells (BrdU-positive cells), apoptotic cells (TUNEL-positive cells), macrophage (F4/80-positive cells) infiltration, and α-smooth muscle actin (α-SMA) expression. (*A, E, I, and M*) Unmanipulated *Agtr1* +/+ kidneys. (*B, F, J, and N*) *Agtr1* +/+ kidney with surgical UUO. (*C, G, K, and O*) Unmanipulated *Agtr1* −/− kidneys, and (*D, H, L, and P*) *Agtr1* −/− kidneys with surgical UUO. (A–D) BrdU-positive cells are stained in brown. (E–H) TUNEL-positive cells are stained in deep blue. BrdU- or TUNEL-positive cells are increased in number along the tubules of *Agtr1* −/− kidneys and *Agtr1* +/+ kidneys only with surgical UUO. (I–L) F4/80 positive cells are stained in brown. (M–P) α-SMA expression is shown in brown. Infiltration of F4/80-positive cells or expression of α-SMA is observed in abundance in the interstitium that surrounds the tubules of *Agtr1* −/− kidneys and *Agtr1* +/+ kidneys with surgical UUO, but not without surgical UUO. There is no qualitative or quantitative difference between *Agtr1* −/− and *Agtr1* +/+ kidneys, both with complete UUO.

of *Agtr1* −/− kidneys (cortex, 0.94 ± 0.12/400× field; medulla, 1.76 ± 0.08/400× field), whereas α-SMA positivity is substantially less in the wild type with intact ureter (cortex, 0.21 ± 0.03/400× field, $P < 0.001$; medulla, 0.53 ± 0.04/400× field, $P < 0.001$; Figs. 3 and 4). Further analysis revealed that in the wild-type kidneys, surgical UUO increases α-SMA expression in the interstitium of the same regions as *Agtr1* −/− kidneys to levels similar to *Agtr1* −/− kidneys (cortex, 1.22 ± 0.04/400× field; medulla, 1.31 ± 0.08/400× field).

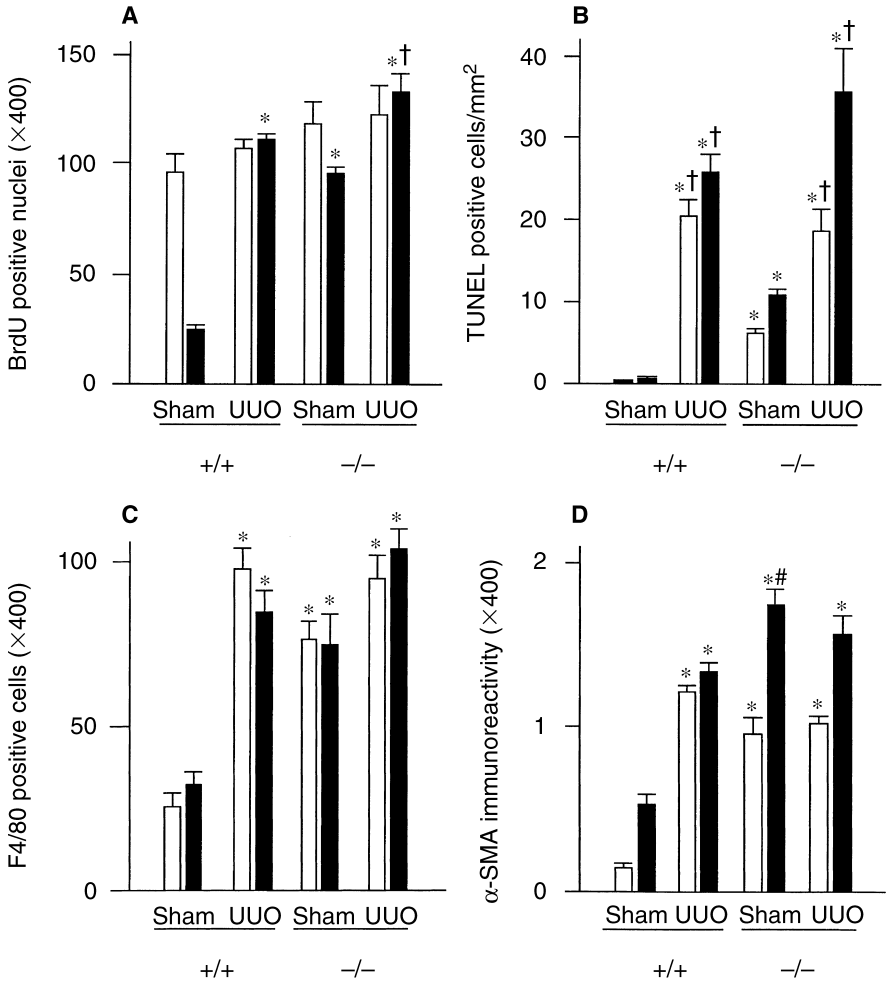

Fig. 4. Quantitative analyses for proliferating cells, apoptotic cells, macrophage infiltration, and α-SMA expression. (*A*) represents number of BrdU positive nuclei in cortex (□) or medulla (■). In the medulla, but not in the cortex, BrdU-positive nuclei are increased in *Agtr1* −/− kidneys to a level similar to *Agtr1* +/+ kidneys with surgical UUO. (*B*) TUNEL-positive cells are higher in number in *Agtr1* −/− kidneys than those in unmanipulated *Agtr1* +/+ kidneys in both cortex and medulla, although lower than those in *Agtr1* +/+ kidneys with UUO. Macrophage infiltration (*C*) and α-SMA expression (*D*) are higher in *Agtr1* −/− kidneys than those in unmanipulated *Agtr1* +/+ kidneys and comparable to *Agtr1* +/+ kidneys with UUO in both cortex and medulla. Values are expressed as mean ± SE. $*P < 0.01$ vs. unmanipulated *Agtr1* +/+ ; $\dagger P < 0.05$ vs. unmanipulated *Agtr1* −/−; $\#P < 0.05$ vs. *Agtr1* +/+ kidneys with UUO.

Expression of transforming growth factor-β1, platelet-derived growth factor, insulin-like growth factor 1, and epidermal growth factor

It has been shown that surgical UUO alters the expression of some growth factors in rodents; for example, TGF-β1 is up-regulated [21, 26], whereas EGF is down-regulated [27]. To ascertain that similar alterations in growth factor expression take place in *Agtr1* −/− kidneys, TGF-β1, PDGF-A, IGF-1, and EGF expressions were examined by a combination of Northern blot analysis, *in situ* hybridization, and immunohistochemistry. As shown in Figure 5, Northern blot analysis revealed that in both *Agtr1* −/− and *Agtr1* +/+ with surgical UUO, the levels of TGF-β1 (*Agtr1* −/−, 2.8-fold; *Agtr1* +/+ with UUO, 6.9-fold, mean values relative to those of *Agtr1* +/+ without UUO), PDGF-A (2.3-fold, 3.3-fold), and IGF-1 mRNAs (1.8-fold, 2.5-fold) are significantly higher, and the level of EGF mRNA expression is significantly lower (*Agtr1* −/−, 0.52; *Agtr1* +/+ with UUO, 0.29) than those of *Agtr1* +/+ kidneys without UUO.

In situ hybridization revealed that the specific signals for both TGF-β1 and PDGF-A mRNAs are present in the areas of interstitial fibrosis that surround dilated tubules in *Agtr1* −/− and *Agtr1* +/+ kidneys with surgical UUO (Fig. 6), whereas *Agtr1* +/+ kidneys without UUO have no appreciable signals for TGF-β1 and weak signals for PDGF-A in the papilla. Immunostaining for IGF1 revealed that IGF1 was weakly positive in the proximal tubules within the deep cortex of *Agtr1* +/+ kidneys without UUO, and the IGF1 immunoreactivity was intensified and extended to the superficial cortical area in both *Agtr1* −/− and *Agtr1* +/+ kidneys with surgical UUO (Fig. 6). In addition, intense EGF immunoreactivity is present in the distal tubules of *Agtr1* +/+ kidneys without UUO, contrasting to the decreased intensity in the immunoreactivity in both *Agtr1* −/− and *Agtr1* +/+ kidneys with UUO (Fig. 6).

Examination for *Agtr1* −/− kidney undergoing complete surgical obstruction

All of the parameters measured and described earlier here in *Agtr1* −/− kidneys are qualitatively similar to those

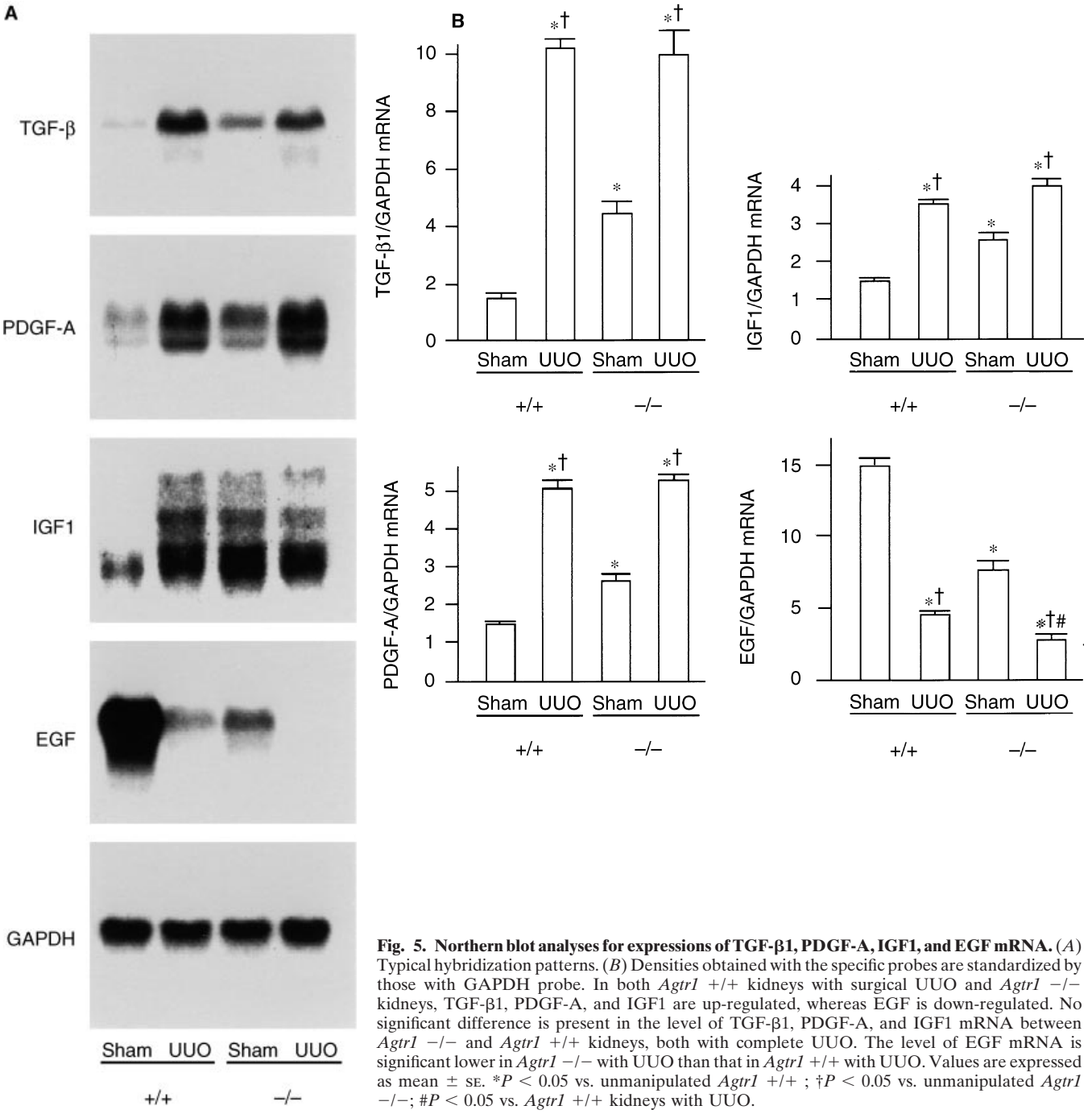

Fig. 5. Northern blot analyses for expressions of TGF-β1, PDGF-A, IGF1, and EGF mRNA. (*A*) Typical hybridization patterns. (*B*) Densities obtained with the specific probes are standardized by those with GAPDH probe. In both *Agtr1* +/+ kidneys with surgical UUO and *Agtr1* −/− kidneys, TGF-β1, PDGF-A, and IGF1 are up-regulated, whereas EGF is down-regulated. No significant difference is present in the level of TGF-β1, PDGF-A, and IGF1 mRNA between *Agtr1* −/− and *Agtr1* +/+ kidneys, both with complete UUO. The level of EGF mRNA is significant lower in *Agtr1* −/− with UUO than that in *Agtr1* +/+ with UUO. Values are expressed as mean ± SE. $*P < 0.05$ vs. unmanipulated *Agtr1* +/+ ; $\dagger P < 0.05$ vs. unmanipulated *Agtr1* −/−; $\#P < 0.05$ vs. *Agtr1* +/+ kidneys with UUO.

in *Agtr1* +/+ with surgically induced complete UUO. To test whether the quantitative differences that exist in these parameters between the two mouse groups are attributed merely to the degree of completeness of urinary tract obstruction and not to a fundamental difference in the pathophysiology leading to the renal lesions, we surgically created a complete UUO in *Agtr1* −/− mice and subsequently repeated assessments for all of these parameters.

Although the levels of BrdU incorporation are somewhat higher in the *Agtr1* −/− kidneys with UUO (cortex, 121.2 ± 16.0/400× field; medulla, 133.0 ± 10.0/400× field, $N = 5$) than that in *Agtr1* +/+ kidneys with UUO (cortex, 107.7 ± 3.6; medulla, 112.5 ± 3.2, $N = 6$), the difference is not statistically significant. Likewise, the number of apoptotic cells is similar during UUO in *Agtr1* −/− (cortex, 18.4 ± 4.6/mm^2; medulla, 36.1 ± 6.7/mm^2, $N = 5$) and *Agtr1* +/+ kidneys (cortex, 20.5 ± 3.3; medulla, 26.0 ± 2.9, $N = 6$; Figs. 3 and 4).

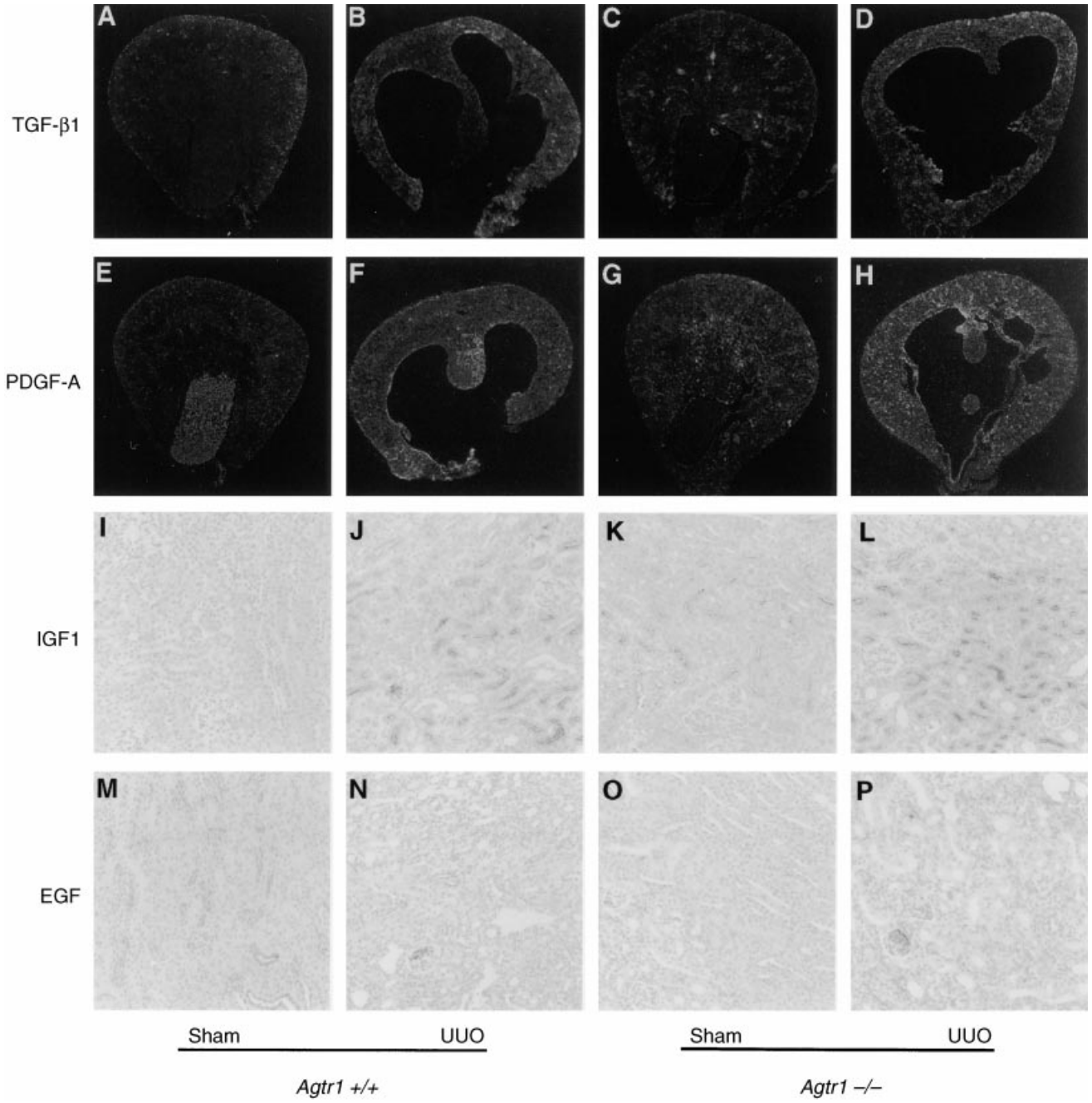

Fig. 6. ***In situ*** **hybridization for TGF-β1 and PDGF-A mRNA and immunohistochemistry for IGF1 and EGF.** (*A, E, I, and M*) Unmanipulated *Agtr1* +/+ kidneys. (*B, F, J, and N*) *Agtr1* +/+ kidney with surgical UUO. (*C, G, K, and O*) Unmanipulated *Agtr1* −/− kidneys, and (*D, H, L, and P*) *Agtr1* −/− kidneys with surgical UUO. Signals for TGF-β1 mRNA (A–D) and PDGF-A mRNA (E–H) are shown by dark field photographs in lower magnifications. Both signals are present in the areas of interstitial fibrosis in *Agtr1* −/− and *Agtr1* +/+ kidney with surgical UUO. Note that PDGF-A mRNA is detected in the papillary region of *Agtr1* +/+ kidneys and not of *Agtr1* −/− kidneys. (*I–L*) Immunoreactive IGF1 is shown in brown. IGF1 is weakly positive in the proximal tubules of the *Agtr1* +/+ kidney without UUO. The immunoreactivity is intensified in the *Agtr1* −/− and *Agtr1* +/+ kidneys with surgical UUO. (*M–P*) Intense EGF immunoreactivity is present in the distal tubules of the *Agtr1* +/+ kidney without UUO. The immunoreactivity decreases in both *Agtr1* −/− and *Agtr1* +/+ kidneys with surgical UUO. There is no qualitative or quantitative difference between *Agtr1* −/− and *Agtr1* +/+ kidneys, both with complete UUO, except for PDGF-A expression in the papilla.

With regards to the papilla to calyx ratio, macrophage infiltration, α-SMA immunoreactivity in the interstitium, and the expression levels of TGF-β1, PDGF-A, IGF1, there is no quantitatively appreciable difference between *Agtr1* −/− and *Agtr1* +/+ when both carry complete UUO (papilla to calyx ratio: *Agtr1* −/−, 26.7 ± 2.6%; *Agtr1* +/+ , 18.3 ± 2.7%; macrophage infiltration in the cortex: *Agtr1* −/−, 99.9 ± 9.6; *Agtr1* +/+ , 97.8 ± 8.5/

400× field; in the medulla: *Agtr1* −/−, 105.5 ± 6.7; *Agtr1* +/+ , 83.8 ± 8.6/400× field; α-SMA in the cortex: *Agtr1* −/−, 1.03 ± 0.05; *Agtr1* +/+ , 1.23 ± 0.05/400× field; in the medulla: *Agtr1* −/−, 1.58 ± 0.1, *Agtr1* +/+ , 1.31 ± 0.08/400× field; TGF-β1 expression, *Agtr1* −/−, 3.8 ± 0.3; *Agtr1* +/+ , 4.5 ± 0.3; PDGF-A expression: *Agtr1* −/−, 3.2 ± 0.3; *Agtr1* +/+ , 2.8 ± 0.3; IGF1 expression: *Agtr1* −/−, 2.2 ± 0.2; *Agtr1* +/+ , 1.9 ± 0.2; EGF expression: *Agtr1* −/−, 0.25 ± 0.06; *Agtr1* +/+ , 0.33 ± 0.07; Figs. 2–6).

Among the parameters tested, only the level of EGF expression was significantly lower in *Agtr1* −/− with UUO (2.4 ± 0.4) than in *Agtr1* +/+ with UUO (4.3 ± 0.5, $P < 0.05$; Fig. 5).

Examination of wild-type kidneys with pharmacological angiotensin-converting enzyme inhibition after birth

We next examined the kidneys of neonatal wild-type mice that had been given ACE inhibitor in order to ascertain that the anomalous kidney development reported under this condition [5, 6] is also attributable to those mechanisms currently investigated for *Agtr1* −/− mice. As shown in Figure 7, the morphology of the upper urinary tract is markedly distorted in wild-type kidneys subjected to pharmacological ACE inhibition (ACEI). Similar to *Agtr1* −/− kidneys, the ampulla-shaped pelvis is absent in these mice at 21 days of age. Moreover, the renal parenchymal damages are characterized by atrophic papilla with dilated calyx, increased BrdU incorporation, apoptotic activity, macrophage infiltration, and α-SMA expression in the interstitium (Fig. 7). In addition, in neonatal mice subjected to ACE inhibition for five days, BrdU incorporation within the pelvic smooth muscle is significantly less in number than that in the control mice (control, 16.2 ± 0.8%, $N = 5$; ACEI 10.3 ± 0.9%, $N = 5$, $P < 0.001$; Fig. 7), whereas renal parenchymal damages, specifically hypoplastic papilla and dilated calyx, were not evident at this time (data not shown).

DISCUSSION

Our study began with the comparison between *Agtr1* −/− kidneys without surgical obstruction and wild-type kidneys with surgical complete UUO with respects to morphometrical, immunohistochemical, and molecular indices. In an earlier pilot study, although the expression of EGF mRNA was somewhat lower in *Agtr1* −/− kidneys when compared with unmanipulated wild-type kidneys, there was no appreciable abnormality in other parameters, for example, gross morphology, BrdU incorporation, apoptotic activity, and the expression patterns of the TGF-β1, PDGF-A, and IGF1 mRNA in *Agtr1* −/− kidneys at postnatal day 16 (P16). However, differences became evident at postnatal day 21 (P21). For this reason, we chose P16 for creating UUO in wild-type mice and P21 for analyzing these various parameters in the kidneys.

These analyses revealed that the nature of the structural anomalies in mutant kidneys are qualitatively indistinguishable from wild-type kidneys with obstruction created experimentally by ureteral ligation. Thus, in both the mutant and artificially obstructed wild-type kidneys, the calyx is enlarged, whereas the papilla is atrophic, and tubulointerstitial cells are not only abnormally apoptotic but also proliferative. Both are also characterized by interstitial macrophage infiltration and fibrosis, and within the local fibrotic area, TGF-β1, PDGF-A, and IGF-1 are up-regulated, whereas EGF is down-regulated as determined by both Northern blot analysis and histological examination. All of these changes documented in this study are identical to those in rats with five day UUO [21, 26−29]. Of interest, TGF-β1 mRNA expression was reported to be down-regulated in neonatal rat kidneys subjected to ACE inhibition [30], whereas the same parameter was found up-regulated in the mutant mice lacking type 1 receptor (*Agtr1* −/−) or angiotensinogen (*Agt* −/−) [7].

Overall, a close similarity was found to exist in this study between *Agtr1* −/− kidneys and experimentally obstructed wild-type kidneys; however, the mutant kidneys have some distinctive features that are not present in the obstructed wild-type kidneys. Thus, mutant kidneys carry renal vascular hypertrophy, whereas these vascular changes are absent in the wild-type kidneys with UUO at 21 days old and even in neonatal kidneys subjected to surgical UUO (data not shown). In addition, *in situ* hybridization for PDGF-A mRNA revealed that distinctive positive signals are present in the papillary region in wild-type mice, regardless of the presence or absence of ureteral ligation, whereas mutant kidneys lack the expression of PDGF-A mRNA in this area (Fig. 6) [7]. These differences indicate the concurrent presence of other pathophysiological processes unique to *Agtr1* −/− kidneys. With these exceptions, all of the parameters measured and described earlier here in *Agtr1* −/− kidneys are qualitatively identical to those in *Agtr1* +/+ with surgically induced complete UUO. In the next set of experiments, we examined whether the quantitative differences that exist between these two kidneys are attributed to the degree of completeness of urinary tract obstruction, as that of *Agtr1* −/− is "partial," whereas that of the wild type is complete. For this purpose, we surgically induced a complete UUO in *Agtr1* −/− and duplicated the previously described measurements. Theoretically, for the same purpose, one may consider a removal of "presumed obstruction" in *Agtr1* −/− mice by surgically creating a vent along the upper urinary tract. This approach is not feasible because we found that nephrostomy closes spontaneously shortly after sur-

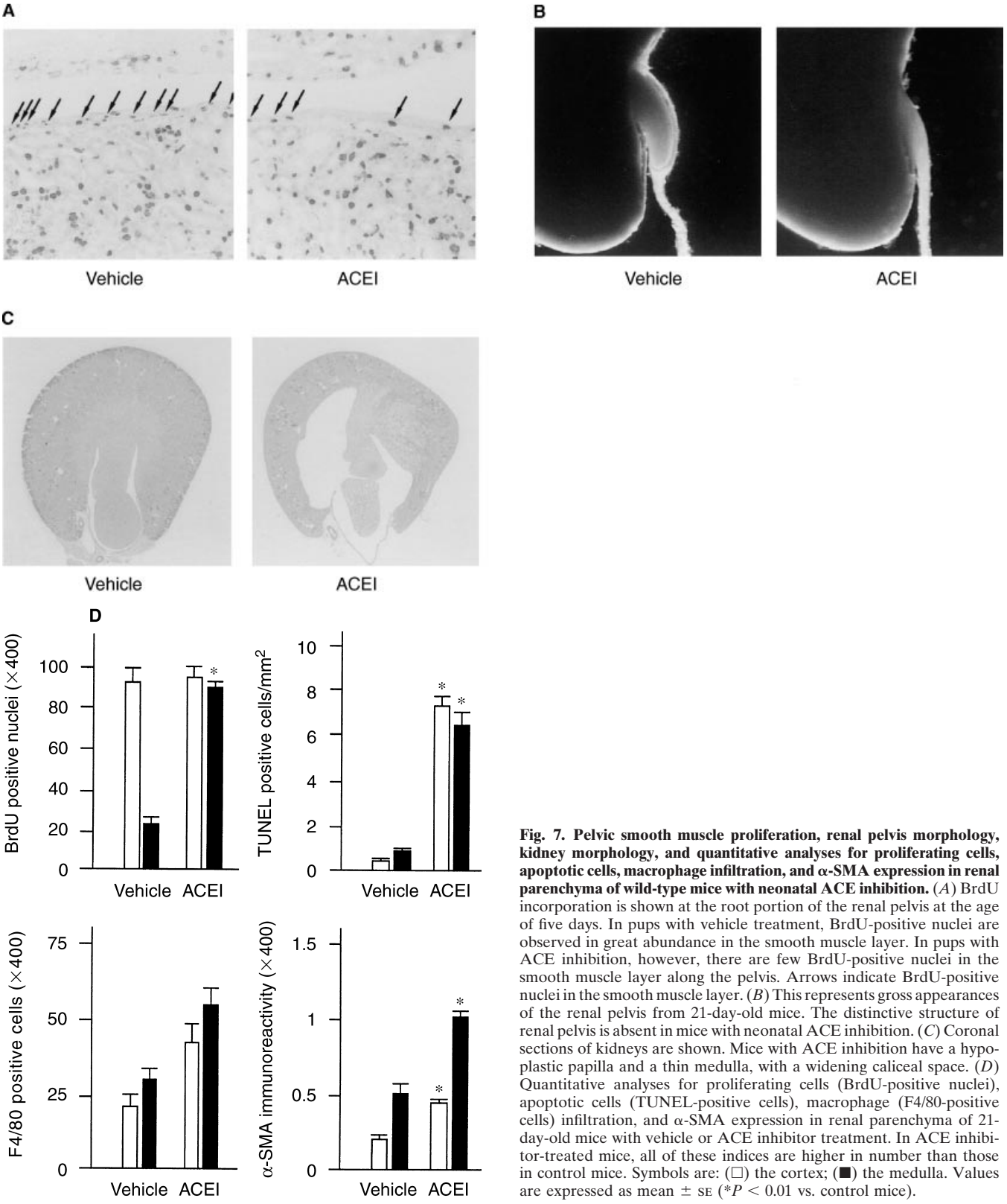

Fig. 7. Pelvic smooth muscle proliferation, renal pelvis morphology, kidney morphology, and quantitative analyses for proliferating cells, apoptotic cells, macrophage infiltration, and α-SMA expression in renal parenchyma of wild-type mice with neonatal ACE inhibition. (*A*) BrdU incorporation is shown at the root portion of the renal pelvis at the age of five days. In pups with vehicle treatment, BrdU-positive nuclei are observed in great abundance in the smooth muscle layer. In pups with ACE inhibition, however, there are few BrdU-positive nuclei in the smooth muscle layer along the pelvis. Arrows indicate BrdU-positive nuclei in the smooth muscle layer. (*B*) This represents gross appearances of the renal pelvis from 21-day-old mice. The distinctive structure of renal pelvis is absent in mice with neonatal ACE inhibition. (*C*) Coronal sections of kidneys are shown. Mice with ACE inhibition have a hypoplastic papilla and a thin medulla, with a widening caliceal space. (*D*) Quantitative analyses for proliferating cells (BrdU-positive nuclei), apoptotic cells (TUNEL-positive cells), macrophage (F4/80-positive cells) infiltration, and α-SMA expression in renal parenchyma of 21-day-old mice with vehicle or ACE inhibitor treatment. In ACE inhibitor-treated mice, all of these indices are higher in number than those in control mice. Symbols are: (□) the cortex; (■) the medulla. Values are expressed as mean ± SE (*$P < 0.01$ vs. control mice).

gery in part because of the lack of constant peristaltic movement of flow through the nephrostomy. Because, in *Agtr1* −/− mice, lack of peristalsis prevails along the entire length of the urinary tract, it is expected that complete removal of the "presumed obstruction" is not possible experimentally.

The chronic ischemic process, for instance, is expected to involve renal parenchymal damage, for example, tubule cell proliferation and apoptosis, interstitial inflammation and fibrosis, up-regulation of TGF-β1, and/or down-regulation of EGF during tissue remodeling [31]. When a complete UUO was created in mutant kidneys, the abnormal values in these kidneys became virtually identical quantitatively to those in wild-type kidneys with the same complete UUO; that is, mutant kidneys are not more severely affected. The difference in the level of EGF mRNA expression that was present between mutant kidneys and nonobstructed wild-type kidneys at the age of 16 days continued to be present after five-day complete UUO in both kidneys. Collectively, based on these qualitative and quantitative analyses, the dilated calyx and atrophic papilla characterizing the kidney of *Agtr1* −/− shortly after birth are attributed primarily to processes that are obstructive in nature.

In addition to the morphological evidence just discussed, we have obtained functional evidence in this study that the urinary tract of *Agtr1* −/− mice is obstructed. We measured the pelvic pressure and the downstream ureteral pressure in the same mice by using the micropuncture servo-nulling method [19]. Although the values for pelvic and ureteral pressure vary somewhat among mice in each group, presumably reflecting the characteristic wide variability in urine flow rate among individual animals [32], the baseline pressure is always lower in the pelvis than in the distal ureter in the wild type, whereas this negative pressure gradient is reversed in mutants. This reversed pressure relationship between the pelvis and ureter pressure is taken as evidence for obstruction in rodents [32]. Because there is no identifiable structural obstruction along the entire urinary tract in *Agtr1* −/− mice, this reversed pressure relationship must imply that the mutant fails to isolate the kidney from downstream high ureteral pressure because of a lack of peristaltic contraction of the urinary tract. This notion is in complete agreement with the lack of renal pelvis and poor ureteral muscle development in *Agtr1* −/− mice reported earlier [4]. Indeed, earlier studies in rats demonstrated that chronic partial ureteral obstruction leads to a constant elevation of distal tubule pressure by some 50% [33].

The patterns of functional abnormalities seen in mice with a defective renin-angiotensin system also duplicate those of animals with partial anatomical obstruction in the urinary tract. Both mild reductions in renal plasma flow rate and glomerular filtration rate, as well as impairments in urine concentrating ability [9, 12], are common to humans and animals with mild urinary tract obstruction [34−36]. These same functional abnormalities were documented in earlier studies in rats given ACE inhibitor during the neonatal period [5, 6].

Angiotensinogen- [7–9] and ACE- [10−12] deficient mice also have renal lesions similar to *Agtr1* −/− mice, including hypoplastic papilla with widening of caliceal space, tubular dilation and atrophy, and interstitial fibrosis [13]. It has been speculated, from these observations, that angiotensin II promotes tubulogenesis directly or regulates the expression of renal growth factor within these areas. In mice, however, no appreciable angiotensin binding site is observed in the papilla and medulla [4, 37], nor is receptor gene promoter activity identified in these areas [13]. Moreover, BrdU incorporation in the tubule cells in the medulla is rather higher in *Agtr1* −/− mice than that in wild-type mice. The renal injury seen in these mice therefore appears to reflect an indirect effect of the inhibition of AT1 function on the renal parenchyma.

We expanded this conclusion to the similar lesions that develop after ACE inhibitor administration in growing animals [5, 6], as the observations were duplicated in wild-type mice that were given an ACE inhibitor since shortly after birth. As shown in Figure 7, in mice given ACE inhibitor after birth, the renal pelvis does not develop properly, and this defect is followed by renal parenchymal damage, a pattern identical to those in *Agtr1* −/− or *Agt* −/− mice [4]. The renal abnormalities seen in these rats and mice therefore are also attributed largely to urinary tract obstruction caused by the lack of the renal pelvis and urinary peristalsis.

In summary, the kidney of neonatal rodents with defective renin-angiotensin system carries functional and structural abnormalities characteristic for obstructed kidneys. This study also revealed that animals that are completely deficient of this system from early embryonic stages carry renal vascular anomalies, which cannot be reproduced by experimental urinary tract obstruction.

ACKNOWLEDGMENTS

This work was supported by National Institutes of Health grants DK-44757 and DK-37868. Dr. Agnes Fogo is a recipient of an Established Investigator Award from the American Heart Association. The authors thank Ms. Teresa Bills and Ms. Ellen Donnert for their technical assistance.

Reprint requests to Iekuni Ichikawa, M.D., Vanderbilt University Medical Center, MCN C4204, 21st and Garland Avenue, Nashville, Tennessee 37232-2584, USA.
E-mail: iekuni.ichikawa@mcmail.vanderbilt.edu

APPENDIX

ACE, angiotensin converting enzyme; ACEI, ACE inhibitor; *Agtr1* −/−, homozygote for null mutations in both the angiotensin type 1 A

and 1B receptor genes; *Agt* −/−, homozygote for null mutation in the angiotensinogen gene; BrdU, bromodeoxyuridine; EGF, epidermal growth factor; GAPDH, glyceraldehyde 3-phosphate dehydrogenase; IGF1, insulin-like growth factor 1; PDGF, platelet-derived growth factor; PFA, paraformaldehyde; SMA, smooth muscle actin; TGF-β1, transforming growth factor beta 1; TUNEL, terminal deoxy transferase uridine triphosphate nick end-labeling; UUO, unilateral ureteral obstruction.

REFERENCES

1. Kotchen TA, Strickland AL, Rice TW, Walters BS: A study of the renin-angiotensin system in newborn infants. *J Pediatr* 80:938–946, 1972
2. Richoux JP, Amsaguine S, Grignon G, Bouhnik J, Menard J, Corvol P: Earliest renin containing cell differentiation during ontogenesis in the rat. *Histochemistry* 88:41–46, 1987
3. Gomez RA, Pupilli C, Everett AD: Molecular and cellular aspects of renin during kidney ontogeny. *Pediatr Nephrol* 5:80–87, 1991
4. Miyazaki Y, Tsuchida S, Nishimura H, Pope JC, Harris RC, McKanna JM, Inagami T, Hogan BLM, Fogo A, Ichikawa I: Angiotensin induces urinary peristaltic machinery during the perinatal period. *J Clin Invest* 102:1489–1497, 1998
5. Friberg P, Sundelin B, Bohman S-O, Bobik A, Nilsson H, Wickman A, Gustafsson H, Petersen J, Adams MA: Renin-angiotensin system in neonatal rats: Induction of a renal abnormality in response to ACE inhibition or angiotensin II antagonism. *Kidney Int* 45:485–492, 1994
6. Guron G, Adams MA, Sundelin B, Friberg P: Neonatal angiotensin converting enzyme inhibition in the rat induces persistent abnormalities in renal function and histology. *Hypertension* 29:91–97, 1997
7. Niimura F, Labosky PA, Kakuchi J, Okubo S, Yoshida H, Oikawa T, Ichiki T, Naftilan AJ, Fogo A, Inagami T, Hogan BLM, Ichikawa I: Gene targeting in mice reveals a requirement for angiotensin in the development and maintenance of kidney morphology and growth factor regulation. *J Clin Invest* 96:2947–2954, 1995
8. Nagata M, Tanimoto K, Fukamizu A, Kon Y, Sugiyama F, Yagami K, Murakami K, Watanabe T: Nephrogenesis and renovascular development in angiotensinogen-deficient mice. *Lab Invest* 75:745–753, 1996
9. Okubo S, Niimura F, Matsuzaka T, Fogo A, Hogan BLM, Ichikawa I: Angiotensinogen gene null-mutant mice lack homeostatic regulation of glomerular filtration and tubular reabsorption. *Kidney Int* 53:617–625, 1998
10. Krege JH, John SWM, Langenbach LL, Hodgin JB, Hagaman JR, Bachman ES, Jennette JC, O'Brien DA, Smithies O: Male-female differences in fertility and blood pressure in ACE-deficient mice. *Nature* 375:146–148, 1995
11. Carpenter C, Honkanen AA, Mashimo H, Goss KA, Huang P, Fishman MC, Asaad M, Dorso CR, Cheung H-S: Renal abnormalities in mutant mice. (letter) *Nature* 380:292, 1996
12. Esther CR, Howard TE, Marino EM, Goddard JM, Capecchi MR, Bernstein KE: Mice lacking angiotensin-converting enzyme have low blood pressure, renal pathology, and reduced male fertility. *Lab Invest* 74:953–965, 1996
13. Tsuchida S, Matsuzaka T, Chen X, Okubo S, Niimura F, Nishimura H, Fogo A, Utsunomiya H, Inagami T, Ichikawa I: Murine double nullizygotes of the angiotensin type 1A and 1B receptor genes have all the major abnormal phenotypes of angiotensinogen nullizygotes. *J Clin Invest* 101:755–760, 1998
14. Boylan BJW, Colbourn EP, McCance RA: Renal function in the foetal and new-born guinea-pig. *J Physiol* 141:323–331, 1958
15. Constantinou CE: Renal pelvic pacemaker control of peristaltic rate. *Am J Physiol* 226:1413–1419, 1974
16. Constantinou CE, Hrynczuk JR: Urodynamics of the upper urinary tract. *Invest Urol* 14:233–240, 1976
17. Gasc J-M, Shanmugam S, Sibony M, Corvol P: Tissue-specific expression of type 1 angiotensin II receptor subtypes: An in situ hybridization study. *Hypertension* 24:531–537, 1994
18. Finberg JPM, Peart WS: Function of smooth muscle of the rat renal pelvis-response of the isolated pelvis muscle to angiotensin and some other substances. *Br J Pharmacol* 39:373–381, 1970
19. Yoshida Y, Fogo A, Ichikawa I: Glomerular hemodynamic changes vs. hypertrophy in experimental glomerular sclerosis. *Kidney Int* 35:654–660, 1989
20. Gavrieli Y, Sherman Y, Ben-Sasson SA: Identification of programmed cell death in situ via specific labeling of nuclear DNA fragmentation. *J Cell Biol* 119:493–501, 1992
21. Kaneto H, Morrissey J, Klahr S: Increased expression of TGF-β1 mRNA in the obstructed kidney of rats with unilateral ureteral ligation. *Kidney Int* 44:313–321, 1993
22. Pelton RW, Dickinson ME, Moses HL, Hogan BLM: In situ hybridization analysis of TGFβ3 RNA expression during mouse development: Comparative studies with TGFβ1 and β2. *Development* 110:609–620, 1990
23. Mercola M, Wang CY, Kelly J, Brownlee C, Jackson-Grusby L, Stiles C, Bowen-Pope D: Selective expression of PDGF-A and its receptor during early mouse embryogenesis. *Dev Biol* 138:114–122, 1990
24. Scott J, Urdea M, Quiroga M, Sanchez-Pescador R, Fong N, Selby M, Rutter WJ, Bell GI: Structure of a mouse submaxillary messenger RNA encoding epidermal growth factor and seven related proteins. *Science* 221:236–241, 1983
25. Bell GI, Stempien MM, Fong NM, Rall LB: Sequences of liver cDNAs encoding two different mouse insulin-like growth factor I precursors. *Nucleic Acids Res* 14:7873–7882, 1986
26. Diamond JR, Kees-Folts D, Ding G, Frye JE, Restrepo NC: Macrophages, monocyte chemoattractant peptide-1, and TGF-β1 in experimental hydronephrosis. *Am J Physiol* 266:F926–F933, 1994
27. Walton G, Buttyan R, Garcia-Montes E, Olsson CA, Hensle TW, Sawczuk IS: Renal growth factor expression during the early phase of experimental hydronephrosis. *J Urol* 148:510–514, 1992
28. Truong LD, Petrusevska G, Yang G, Gurpinar T, Shappell S, Lechago J, Rouse D, Suki WN: Cell apoptosis and proliferation in experimental chronic obstructive uropathy. *Kidney Int* 50:200–207, 1996
29. Chevalier RL: Growth factors and apoptosis in neonatal ureteral obstruction. *J Am Soc Nephrol* 7:1098–1105, 1996
30. Yoo KH, Wolstenholme JT, Chevalier RL: Angiotensin-converting enzyme inhibition decreases growth factor expression in the neonatal rat kidney. *Pediatr Res* 42:588–592, 1992
31. Shanley PF: The pathology of chronic renal ischemia. *Semin Nephrol* 16:21–32, 1996
32. Fichtner J, Boineau FG, Lewy JE, Sibley RK, Vari RC, Shortliffe LMD: Congenital unilateral hydronephrosis in a rat model: Continuous renal pelvic and bladder pressures. *J Urol* 152:652–657, 1994
33. Ichikawa I, Brenner BM: Local intrarenal vasoconstrictor-vasodilator interactions in mild partial ureteral obstruction. *Am J Physiol* 236:F131–F140, 1979
34. Kekomaki M, Wehle M, Walker RD: The growing rabbit with a solitary, partially-obstructed kidney: Analysis of an experimental model with reference to the renal concentrating ability. *J Urol* 133:870–872, 1985
35. Bratt C-G, Aurell M, Jonsson O, Nilsson S: Long-term followup of maximum concentrating ability and glomerular filtration rate in adult obstructed kidneys after pyeloplasty. *J Urol* 140:273–276, 1988
36. Kinn AC: Renal function in idiopathic hydronephrosis. *Scand J Urol Nephrol* 17:169–174, 1983
37. Ito M, Oliverio MI, Mannon PJ, Best CF, Maeda N, Smithies O, Coffman TM: Regulation of blood pressure by the type 1A angiotensin II receptor gene. *Proc Natl Acad Sci USA* 92:3521–3525, 1995